A Missing Piece of the Puzzle in Pulmonary Fibrosis: Anoikis Resistance Promotes Fibroblast Activation

Juan Yin
Southeast University
Jing Wang
Southeast University
Xinxin Zhang
Southeast University
Yan Liao
Southeast University
Wei Luo
Southeast University
Sha Wang
Southeast University
Jiawei Ding
Southeast University
Jie Huang
Southeast University
Mengling Chen
Southeast University
Wei Wang
Southeast University
Shencun Fang
Southeast University
Jie Chao (chaojie@seu.edu.cn)
Southeast University https://orcid.org/0000-0002-7800-3557

Research

Keywords: Anoikis, ZC3H4, pulmonary fibrosis, fibroblast, ECM

Posted Date: October 20th, 2021

DOI: https://doi.org/10.21203/rs.3.rs-968663/v1

Version of Record: A version of this preprint was published at Cell & Bioscience on February 25th, 2022. See the published version at https://doi.org/10.1186/s13578-022-00761-2.

Abstract

Background Pulmonary fibrosis initiates a pneumonic cascade that leads to the dysfunction of fibroblasts characterized by excess proliferation. Anoikis is a physiological process that ensures tissue development and homeostasis. Whether disruption of anoikis is involved in pulmonary fibrosis remains unclear.

Results Here, we investigated the mechanism by which silica induces fibroblast activation via anoikis resistance in the subsequent fibrosis. Anoikis of lung fibroblasts, alveolar epithelial cells and endothelial cells during the process of fibrosis was detected by CCK-8, western blot, cell count and flow cytometry (FCM) assays. While the three cell types showed similar increases in cell proliferation, the expression of NTRK2, a marker of anoikis resistance, was upregulated specifically in fibroblasts, indicating the unique proliferative mechanism of fibroblasts in pulmonary fibrosis, which may be related to anoikis resistance. Furthermore, the CRISPR/Cas9 system was used to investigate the molecular mechanism of anoikis resistance; the SiO_2-induced inflammatory response activated the MAPK/PI3K signaling pathway in lung fibroblasts and then induced the protein expression of ZC3H4, which specifically mediated anoikis resistance, followed by pulmonary fibrosis.

Conclusion The current study revealed a specific pattern of fibroblast proliferation, and targeting anoikis resistance may inhibit the pathological process of pulmonary fibrosis. This result provides a new approach for treating pulmonary fibrosis and new insights for the potential application of ZC3H4 in the development of novel therapeutic strategies for mitigating pulmonary fibrosis.

Introduction

Pulmonary fibrosis is a kind of lung disease caused by abnormal wound healing in susceptible people with repeated injury of alveoli. This condition mainly manifests as chronic inflammation and collagen deposition in the extracellular matrix (ECM), which eventually lead to diminished lung function, and is the final step of many lung diseases [1, 2]. This process is characterized by continuous and irreversible damage and involves a variety of lung cells such as fibroblasts [3], epithelial cells [4], and endothelial cells. To date, pulmonary fibrosis has not been fully elucidated. The excessive proliferation of lung cells during pulmonary fibrosis is similar to the proliferation of detached cells caused by anoikis resistance during tumor invasion or migration and skin injury [5]. Anoikis, first identified in 1993, is a unique programmed death phenomenon caused by adherent cells leaving the ECM [6]. The ECM is a complex multimolecular protein network that provides structural support for cells and serves as an adherent substrate for cell migration [7]. During the processes of angiogenesis and wound healing, reshaping of the ECM is essential and can be regarded as a physiological process to ensure appropriate tissue development and homeostasis [7]. The dynamic balance between cells and the surrounding microenvironment is maintained by preventing detached cells from reattaching to a new matrix and growing in the wrong place [8]. Thus, failure to execute the anoikis program may result in detached cells surviving in a suspension or proliferating at ectopic sites in the ECM that differ from the primary matrix.

Removing the restriction on anoikis execution was identified as a hallmark of malignancy and facilitates the survival of cancer cells in the circulatory system to complete their metastasis to distant organs [9, 10]. Previous studies have shown that the zinc finger protein MCP-1 inducible protein (MCPIP1) and the newly discovered zinc finger protein ZC3H4 are involved in fibrosis [11]. MCPIP1 (also known as ZC3H12A) is involved in silica-induced pulmonary fibrosis and regulates macrophage and fibroblast activation [12]. ZC3H4 and MCPIP1 belong to the CCCH-type zinc finger protein family. In RAW264.7 mouse macrophages, ZC3H4 promoted the activation of macrophages and downstream fibroblasts [13]. In the current study, the zinc finger protein ZC3H4 was shown to promote anoikis resistance in fibroblasts and subsequently induce pulmonary fibrosis. These findings reveal a novel role of anoikis in silica-induced pulmonary inflammation and suggest that ZC3H4 is a target for the clinical diagnosis and treatment of pulmonary fibrosis.

Materials And Methods

Reagents

Silicon dioxide, in which 80% of particles exhibited a diameter of less than 5 μm, was purchased from Sigma® (S5631), processed via sedimentation according to Stokes' law, subjected to acid hydrolysis, and baked overnight (200°C for 16 h) [14]. Antibodies against ZC3H4 (2004 1-1-AP, rabbit), TrkB (13129-1-AP, rabbit), BIP (11578-1-AP, rabbit), CHOP (15204-1-AP, rabbit), ATF6α (66563-1-AP, mouse), ATG5 (60061-1-AP, mouse), BECN1 (11306-1-AP, rabbit), and LC3B (14600-1-AP, rabbit) were purchased from Proteintech, Inc. Antibodies against Akt (4691S, rabbit), p-Akt (4060S, rabbit), JNK (9258S, rabbit), p-JNK (4668S, rabbit) and IRE1α (3294, rabbit) were purchased from CST, Inc. Antibodies against GAPDH (sc-25778, rabbit) and NPNT (393033, rabbit) were purchased from Santa Cruz, Inc.

Cell culture

BEAS-2B, HPMECs and THP-1 cells were purchased from ATCC®. Human pulmonary fibroblasts from adults (HPF-a), mouse pulmonary fibroblasts (MLG) and RAW264.7 cells were purchased from ScienCell and maintained in DMEM containing 10% FBS at 5% CO_2 and 37°C in an incubator (Thermo Heracell 150i CO_2 incubator, Thermo Fisher Scienti□c, Inc., Germany).

Establishment of a mouse model of silicosis

The mouse model of silicosis was established as previously described [15]. All experiments were approved by the Institutional Animal Care and Use Committee of the Medical School of Southeast University.

Spatial transcriptomics (GSE183683)

1 Sample collection

For the model group, the inclusion criteria were same as those for single-cell sequencing. Lung tissues were sliced appropriately in the horizontal direction and then frozen in OCT on dry ice as quickly as possible.

2 Staining and imaging

Cryosections were sliced at a thickness of 10 μm and mounted onto the GEX arrays. They were then placed on a Thermocycler Adaptor with the active surface facing up and incubated for 1 min at 37°C. Afterward, the sections were fixed for 30 min with methylalcohol at -20°C and subjected to staining with H&E (Eosin, Dako CS701, Hematoxylin Dako S3309, bluing buffer CS702). Brightfield images were taken on a Leica DMI8 whole-slide scanner at 10x resolution.

3 Permeabilization and reverse transcription

Visium spatial gene expression was processed using a Visium spatial gene expression slide and reagent kit (10x Genomics, PN-1000184). For each well, a slide cassette was used to create leakproof wells to allow the addition of reagents. First, 70 μl of permeabilization enzyme was added and incubated with the sections at 37°C. For NS-7d, SiO2-7d and NS-56d, the incubation time lasted 24 min; for SiO2-56d, the incubation lasted for 30 min to induce severe lung fibrosis. Each well was washed with 100 μl of SSC, and 75 μl of RT master mix was added for cDNA synthesis.

4 cDNA library preparation for sequencing

Upon completion of first-strand synthesis, the RT master mix was removed from the wells and replaced with 75 μl of 0.08 M KOH. After an incubation of 5 min at room temperature, the KOH was aspirated from the wells, and the slices were washed with 100 μl of EB buffer before 75 μl of Second Strand Mix was added to each well for second-strand synthesis. cDNA amplification was performed on a S1000TM Touch Thermal Cycler (Bio Rad). Visium spatial libraries were constructed using the Visium spatial library construction kit (10x Genomics, PN-1000184) according to the manufacturer's instructions. The final libraries were sequenced using an Illumina NovaSeq 6000 sequencer with a sequencing depth of at least 100,000 reads per spot with a pair-end 150 bp (PE150) reading strategy (performed by CapitalBio Technology, Beijing).

Proteomic analysis of the ECM (PXD028194)

1 Experimental procedures

Total protein was extracted from 6 lung ECM samples (3 for the NS-56d group, namely, con111, con116, con117; 3 for the SiO_2-56d group, namely, M80, M101, M107), and a portion (10 μl) of the protein was used to measure the protein concentration, followed by SDS-PAGE separation. Another part was collected for trypsin digestion and labelled with TMT (Tandem Mass Tags) reagents, con111 with 126, con 116 with 127, con117 with 128; M80 with 129, M101 with 130, M107 with 131. Equal amounts of each labelled sample were mixed, and an appropriate quantity of protein was taken to perform

chromatographic separation. Finally, the samples were analysed by LC-MS (liquid chromatography mass spectrometry).

2 Analysis of LC-MS/MS data

The LC-MS/MS raw data was processed using Proteome Discover 2.4 (Thermo, USA). According to the unique peptide ≥ 1, keep any group of samples with the expression value ≥ 50% of the protein. Then, the missing values were imputed with the mean of the protein expression in corresponding group. Next, the data was median normalized and log2-transformed to obtain credible proteins. Then we performed statistical and visual display of these proteins using R software (version 4.2) ggplot2 package (version 3.2.2), including principal component analysis (PCA), sample correlation analysis, sample hierarchical cluster analysis, visual display of data after standardization and density plot.

Based on credible proteins, we performed Student's t test to identify significant difference of proteins in NS-56d group and SiO_2-56d group. Fold change (FC) is used to evaluate the expression level of a certain protein between samples. The p-value (P) calculated by the t-test shows the significance of the difference between samples. Difference screening conditions are FC≥2.0 and P≤0.05. The clustering heat map based on R software (version 4.2) pheatmap package (version 1.0.12) can be used for quality control of standardized experimental data and data display after enrichment of differential data. Generally, samples of the same group can appear in the same cluster through clustering.

For the identified proteins, extract the annotation information based on such as Uniprot databases. After obtaining the differentially expressed proteins (FC≥2, P≤0.05), the GO and KEGG functional enrichment analyses of up-regulated proteins were performed with R software (version 4.2) ggplot2 package (version 3.2.2).

Bioinfomation analysis-space ranger pipeline

Space Ranger software was obtained from the 10x Genomics website (https://support.10xgenomics.com/spatial-gene-expression/software/downloads/latest). Alignment, filtering, barcode counting, and UMI counting were performed with the Space Ranger Count module to generate a feature-barcode matrix and determine clusters. Dimensionality reduction was performed using principal component analysis (PCA), and the first ten principle components were used to generate clusters with the K-means algorithm and graph-based algorithm, respectively.

CRISPR/Cas9 plasmid transfection technology

Fibroblasts were transiently transfected with CRISPR/Cas9 plasmids according to the manufacturer's recommended protocol (Santa Cruz®) to delete or upregulate ZC3H4 expression and examine the downstream effects. The transfection efficiency was determined via western blotting. In brief, HPF-a cells were seeded at 2× 105 cells per well in a 6-well plate in 3 mL of antibiotic-free standard growth medium and grown to 40-80% confluency. Then, 300 µL of the Plasmid DNA/UltraCruz® Transfection Reagent Complex, consisting of 2 µg of plasmid DNA and 10 µL of the UltraCruz® Transfection Reagent in Plasmid Transfection Medium, was added dropwise to each well. Thereafter, gentle mixing was

performed by swirling the plate, and the cells were incubated for 24-72 h under normal conditions prior to their use in subsequent experiments.

Anoikis model

Poly-2-hydroxyethyl methacrylate (poly-HEMA, Sigma, USA) was prepared with anhydrous ethanol at a concentration of 10 mg/mL. A 1.5 mL poly-HEMA solution was added to a 6-well plate and then dried for 24 h under sterile conditions. The wells coated with poly-HEMA were immediately subjected to ultraviolet light for disinfection and washed twice with sterile PBS. Approximately 5×10^5 cells in a single-cell suspension were added to each well and cultured at 37°C with 5% CO2 for 48 h. The cells were then collected and washed twice with sterile PBS. Flow cytometry (FCM) was used to detect the incidence of anoikis among cells stained with an Annexin V-PE apoptosis assay kit (KeyGEN BioTECH, KGA108, Nanjing, China).

Extracellular matrix model of mouse lung tissue

Tissues were embedded with OCT gel, frozen and sliced into 200 μm sections with a cryotome before they were placed into tissue culture dishes containing 15 mL of lysis solution (prepared with 1% SDS deionized water) for digestion. The solution was then changed to 1% Triton X-100 in deionized water. After the samples were washed with PBS, DNase (20 μg/mL) and MgCl (4.2 mM) were added to the tissue to remove protein. Tissues were sterilized with 0.18% peroxyacetic acid and 4.8% acetic acid for 20 min, washed with sterile PBS three times, and stored at 4°C. Mouse tissues that were approximately the same size were selected and fixed to the bottoms of a 24-well culture plate. HPF-a cells were seeded at 1×10^6 cells on top of the tissues and incubated at 37°C for 1 h. When the cells adhered to the wall, 1 mL of complete medium was prepared. The tissue gel was washed twice with PBS before it was digested with collagenase (5 mg/mL), and the sample was cultured for 2-4 days and then collected for cell counting.

Statistics

The data are presented as the means ± standard error of the mean (SEM). Statistical analyses were performed using Student's t test or two-way analysis of variance (ANOVA) with GraphPad 8.0. The tests used are indicated in the figure legends. The ANOVA results were considered significant at $p < 0.05$.

Results

SiO_2-induced pulmonary inflammation caused anoikis resistance specifically in fibroblasts

The conditioned medium (CM) of alveolar macrophages exposed to SiO_2 were collected and cocultured with lung cells to simulate the silica-stimulated inflammatory environment in the lung. Based on the SiO_2 dose-response relationship experiment conducted by a previous laboratory [13], we set the SiO_2 concentration to 50 μg/cm^2. HPF-a cells were selected to screen the appropriate CM, and CM from

macrophages exposed to SiO_2 for 6 hours induced a significant increase in HPF-a cell viability; thus, this CM was selected for all subsequent experiments (Figure 1A). Then, lung fibroblasts, epithelial cells, and endothelial cells were incubated with CM. As shown in Figure 1B-D, CM treatment increased the activity of all three types of cells (Figure 1B-D), while only fibroblasts exhibited increased expression of the NTRK2 (TrkB, a molecular marker of anoikis resistance) protein, which peaked at 24 and 48 h, under CM stimulation (Figure 1E-G). To validate the *in vitro* findings, we established a mouse model of silicosis. Sirius Red staining showed severe damage to the alveolar cavity and increased collagen deposition in the SiO_2 group, demonstrating the successful establishment of pulmonary fibrosis (Figure 1H). Immunofluorescence staining results showed that the expression level of the fibroblast marker vimentin in lung tissue was increased in the SiO_2 group compared with the normal saline (NS) group, confirming the occurrence of pulmonary fibrosis (Figure 1I). Consistent with the *in vitro* experiments, the expression of NTRK2 in the lung tissue of the SiO_2 group was increased and colocalized with vimentin (Figure 1I). By contrast, a similar pattern did not appear in lung epithelial cells and pulmonary endothelial cells (Supplementary Figure S1), suggesting anoikis resistance uniquely occurred in fibroblasts after CM stimulation. Furthermore, spatial transcriptomics results suggested that *Ntrk2* expression was specifically increased in fibroblasts as indicated by colocalization of *Ntrk2* and *Vimentin* (Figure 1J), confirming anoikis resistance in fibroblasts.

Proliferation, but not apoptosis, contributed to anoikis resistance in fibroblasts

Anoikis is a type of apoptosis in response to inappropriate cell/ECM interactions, indicating a special case of cell death initiated by signals not used in response to other proapoptotic insults. To further elucidate the process of anoikis resistance induced by CM, we used FCM. To our surprise, the CM tended to slightly increase apoptosis in fibroblasts (Figure 2A and B) but induced a significant increase in cell viability (Figure 2C), indicating the anoikis resistance induced by CM may not be due to the decrease in apoptosis. To confirm the role of anoikis resistance in proliferation induced by CM, we used poly-HEMA to establish an *in vitro* anoikis model. Upon culture in the presence of poly-HEMA, the cells no longer adhered to the plate but showed a state of agglomeration and suspension growth (Figure 2D). After 48 h, the cells exhibited obvious apoptosis, and the number of cells seeded in precoated poly-HEMA plates was significantly reduced compared to that in uncoated plates (Figure 2E). Interestingly, the CM-induced slight increase in apoptosis was augmented by poly-HEMA pretreatment (Figure 2F and G), ruling out the role of apoptosis in anoikis resistance. Furthermore, poly-HEMA pretreatment abolished the increase in cell viability induced by CM in fibroblasts, confirming the role of cell proliferation in anoikis resistance. Moreover, this pattern was not observed in the epithelial cells and endothelial cells (Supplementary Figure S2A-D), reinforcing the unique mechanism of fibroblasts in pulmonary fibrosis. To validate the *in vitro* results, colocalization of apoptosis (*Cas3* and *Bim1*, Figure 2I) and proliferation (*Cdk1* and *Ccnb2*, Figure 2J) markers with *Vimentin* was shown, and the levels of proliferation markers was increased significantly in SiO_2 groups. Then, MLG cells were transplanted back into decellularized ECM and exposed to a growth environment of cell nests (Figure 2K). After three days, the cells were recovered and counted. The results

showed that CM promoted cell proliferation, which imitated the *in vivo* environment (Figure 2L). Moreover, cell migration was increased in decellularized ECM treated with CM (Figure 2M-O), indicating the activation of cell, which facilitated spreading of dysfunctional fibroblasts, followed by continuous fibrosis.

ZC3H4 was involved in anoikis resistance in fibroblasts in response to CM

To further understand the molecular mechanism of anoikis resistance, we assessed ZC3H4, a member of the zinc finger protein family, in fibroblasts since ZC3H4 was shown to be involved in pulmonary fibrosis [13, 16]. As shown in Figure 3A and B, ZC3H4 expression was significantly increased and peaked at 6 h. To further determine the role of ZC3H4 in anoikis resistance, we seeded fibroblasts in wells precoated with poly-HEMA, and ZC3H4 expression significantly decreased compared to that in the control group (Figure 3C and D). To clarify the role of ZC3H4 in anoikis resistance, we applied CRISPR/Cas9 technology to specifically knock down ZC3H4 in HPF-a cells (Supplementary Figure S3). As shown in Figure 3E and F, the CM-induced increase in NTRK2 in HPF-a cells was significantly reversed after specific knockdown of ZC3H4, suggesting the important role of ZC3H4 in anoikis resistance. Moreover, the spatial transcriptomics results confirmed the increase in *Zc3h4* expression in fibroblasts as indicted by colocalization with *Vimentin* (Figure 3G).

CM induced endoplasmic reticulum stress, but not autophagy, in HPF-a cells

Next, we investigated endoplasmic reticulum stress (ERS) and autophagy since these processes play an important role in pulmonary fibrosis [15]. First, CM induced significant increases in the expression of ERS markers (BiP, ATF6α, CHOP and IRE1α) (Figure 4A and B). Moreover, after pretreatment with the ERS inhibitor salubrinal, the CM-induced increases in ZC3H4 and NTRK2 were attenuated, suggesting that ERS participates in ZC3H4-mediated anoikis resistance in fibroblasts. Then, the expression of autophagy-related proteins (ATG5, BECN1 and LC3B) was also detected, and none of those markers showed significant changes (Figure 4F-I), ruling out the participation of autophagy in anoikis resistance in fibroblasts.

PI3K/MAPKs were involved in ZC3H4-mediated anoikis resistance in response to SiO_2

To further explore the molecular mechanism by which ZC3H4 expression increases, we also investigated prosurvival signals since they were shown to have an important role in anoikis [17–19], as well as pulmonary fibrosis [15, 18, 20, 21]. The effects of CM on the MAPK and PI3K/Akt pathways in fibroblasts were investigated. As shown in Figure 5A and B, CM induced a rapid and transient phosphorylation of MAPK8/JNK, MAPK1/ERK, MAPK14/p38 and AKT1 (0.25 h), which peaked at 30 or 60 minutes (Figure 5A and B). To confirm the role of the MAPK and PI3K/Akt pathways, we applied specific inhibitors targeting JNK (SP600125), p38 (SB203580) or PI3K (LY294002) to pretreat the fibroblasts, which

reversed the increase in ZC3H4 and NTRK2 levels induced by CM (Figure 5C and D). This finding indicates that the PI3K and MAPK signaling pathways are involved in anoikis resistance via regulation of ZC3H4.

The ECM was involved in the detachment of lung fibroblasts in SiO_2-induced pulmonary inflammation

Having determined the role of the apoptotic process in anoikis resistance, we then investigated the interaction in response to inappropriate ECM. The ECM in the lung not only provides structural support for cells but also plays an important role in organogenesis, injury repair, and homeostasis. Since anoikis is largely caused by decreased adhesion between fibroblasts and the fibrotic ECM, we performed proteomic sequencing of the ECM isolated from the lungs of the saline- and SiO_2-treated mice, and 147 differentially expressed proteins were upregulated and 123 differentially expressed proteins were downregulated (Figure 6A and B). GO analysis showed that the downregulated proteins were mainly involved in the biological process of cell adhesion, and their main components were collagen related (Figure 6C and D). According to KEGG signaling pathway enrichment analysis, the proteins with downregulated expression were highly enriched in mediating ECM-receptor recognition and adhesion-related signaling pathways (Figure 6E). These results suggest that the ECM is involved in the loss of nest cells in the lung tissues of mice with silicosis. To clarify the relationship between ECM and nested cells in lung tissues of silicosis mice, we analyzed the top 20 genes corresponding to the downregulated proteins and found that most of the genes were adhesion related, among which NPNT (a member of the epidermal growth factor (EGF)-like superfamily) showed the greatest downregulated expression. NPNT regulates integrin-mediated signaling through the interaction of its RGD motif with integrin α8β1 [22] and is also involved in regulating cell adhesion, differentiation, diffusion, and survival [23–25]. NPNT expression in the ECM was measured to verify the proteomic results by western blots (Figure 7A) and immunofluorescence staining (Figure 7B). Furthermore, downstream genes of NPNT were identified, among which the levels of *Itga8* (Figure 7D), but not *Itgb1* (Supplementary Figure S4), was decreased in spatial transcriptomics results, indicating that this cascade is mediated by NPNT.

SiO_2-induced pulmonary inflammation facilitated anoikis resistance of fibroblasts attached to ECM

Since the ECM proteomic results suggested that cell detachment might initiate the process of anoikis resistance, whether CM also affects this process needs to be clarified. For ethical reasons, the ECM was isolated from mice, so mouse pulmonary fibroblasts (MLG) were applied in following experiments. The anoikis resistance pattern was confirmed by detection of NTRK2 in MLG exposed to CM from RAW264.7 cells treated with SiO_2. As shown in Figure 7E and F, CM induced a similar increase in NTRK2 in MLG, which peaked at 12 h. Moreover, cell migration was increased both in normal decellularized ECM treated with CM and in decellularized ECM isolated from mouse exposed to SiO_2 for 56 day (Fib-ECM) (Figure 7G-I), which facilitated continuous fibrosis.

Discussion

Pulmonary fibrosis is characterized by excessive fibroblast proliferation and abnormal collagen deposition [1, 4, 8, 18, 26–30], which has similar pathological process to cancer. Although anoikis was shown to have important role in cancer progression [10, 17, 31–33], the role of anoikis in pulmonary fibrosis remains unclear. The current study revealed a unique model of anoikis in pulmonary fibroblasts, which depends on both resistance to anoikis and decreased adherence to the ECM, suggesting a tight connection between fibroblast proliferation and abnormal collagen deposition. These results indicate a vital role of anoikis resistance in fibroblast proliferation during pulmonary fibrosis.

In the current study, silica was applied to establish the pulmonary fibrosis model, which is a typical form of chronic pulmonary fibrosis [34, 35] and mimics the clinical symptoms of fibrosis, such as silicosis. Silicosis is one of the major occupational diseases worldwide and is caused by long-term inhalation of SiO_2, with pulmonary fibrosis as the outcome [36]. Although many studies have been performed, the mechanism of pulmonary fibrosis in silicosis has not yet been established. China has the largest number of silicosis patients in the world, and due to the large population, the number of these patients is increasing annually. Therefore, elucidation of the etiology of silicosis is still underway. Silica-induced pulmonary fibrosis is related to the particle size of SiO_2 inhaled [37]. Compared with most nontoxic nano-SiO_2 particles, micro-scaled SiO_2 particles have a strong ability to induce fibrosis, with fibrotic nodules appearing after 30–60 days in exposed mice. Unfortunately, micron-scaled SiO_2 particles are more common pollutants in occupational environments [34]. In this study, SiO_2 particles with a diameter of approximately 5 μm were used as the main irritant, which helped clarify the specific process of pulmonary fibrosis with a similar mechanism.

Fibroblast proliferation is the main pathological process in pulmonary fibrosis [1, 38, 39] and may be due to either an increase in cell number or a decrease in cell death. A recent study suggested a direct effect of SiO_2 on fibroblast proliferation, which was mainly caused by a decrease in apoptosis of fibroblasts via ERS [40]. Interestingly, CM from macrophages exposed to SiO_2 did not show any significant effect on apoptosis of fibroblasts, indicating a different effect of the inflammatory environment compared to the direct effect of SiO_2 on fibroblasts. Apoptosis mainly occurs in pulmonary macrophages after phagocytosis of silica particles (also known as dust cells), followed by an inflammatory cascade at the early stage. Dust cells undergo apoptosis and release SiO_2 particles again, forming a vicious cycle with the release of inflammatory factors, which leads to alveolar epithelial injury and fibroblast activation [29, 41]. Furthermore, SiO_2 particles in the alveoli that directly contact epithelial cells can cause edema and necrosis [28]. Loss of epithelial cells leads to exposure of the lung interstitium, upon which lung fibroblasts migrate outward and are activated into myofibroblasts under the direct and indirect activities of SiO_2 [39]. Obviously, multiple mechanisms, such as classical apoptosis, necrosis, or ferroptosis, are involved in excessive proliferation of fibroblasts. Notably, as a type of mesenchymal cell, fibroblasts are strongly affected by the environment, such as the ECM. As shown in current study, inflammatory factors released by macrophages exacerbated apoptosis in detached fibroblasts, indicating excessive

proliferation of fibroblasts should be a comprehensive result of direct and indirect effects produced by either macrophages or ECM. Moreover, the specific increase in the anoikis resistance marker NTRK2 suggested a unique interaction between fibroblasts and ECM during pulmonary fibrosis.

Increasing evidence suggested that the ECM can regulate cell function, fate and phenotype in a physiological setting, while the composition and function of the ECM are obviously disordered in pathological tissue remodeling [42]. Anoikis is a physiological protective mechanism to prevent excessive proliferation of fibroblasts detached from ECM [5, 33], which may be caused by disruption of the integrin signaling pathway in fibroblasts [31] or changes in the components within the fibrotic ECM. There are few reports about the global changes of proteins in the ECM during pulmonary fibrosis, and thus, proteomics was utilized to analyze the change in the protein profile of the ECM after SiO_2 exposure. As expected, various proteins involved in mediating cell-ECM adhesions showed downregulated expression, indicating the initiation of anoikis and suggesting that detachment and proliferation in anoikis resistance experienced by fibroblasts are two independent events that need to be investigated separately.

ZC3H4, a novel member of zinc finger protein family, has been shown to play a key role in anoikis resistance in fibroblasts since a recent study suggested a role of zinc finger proteins in anoikis in different conditions [32, 33]; for example, ZNF32 and ZNF304 promoted abnormal tissue repair and mitigated tumor cell metastasis via anoikis resistance. Accordingly, both ZC3H12A and ZC3H4 are involved in progression of pulmonary fibrosis [12, 13, 15, 16, 20], but the connection to anoikis is still unclear. In this study, ZC3H4 was observed to regulate the anoikis resistance of fibroblasts and participate in pulmonary fibrosis. Since both autophagy [43–45] and ERS [46–48] play an important role in the tissue fibrosis, as well regulation of abnormal protein expression, the connection between ZC3H4 and autophagy/ERS was investigated. In addition, the signaling pathway of ZC3H4 was verified, in which MAPK/PI3K signaling promoted anoikis resistance, followed by pulmonary fibrosis.

In summary, SiO_2 induced the synergistic action of macrophage-derived inflammatory factors that promoted detached fibroblasts from the ECM the undergo proliferation, named anoikis resistance, following persistent and irreversible pulmonary fibrosis. ZC3H4 mediated anoikis resistance with ERS and MAPK/PI3K signaling pathway activation (Figure 8). The results of this study suggest that anoikis resistance is highly associated with fibrosis and has abnormal activity during the repair of abnormal lung tissue.

Our study showed that fibroblasts exhibit detachment and anoikis resistance in lung tissues during fibrosis. The zinc finger protein ZC3H4 regulates the development of anoikis resistance in fibroblasts, and its expression is increased during fibrosis. The PI3K and MAPK signaling pathways are activated during pulmonary fibrosis, and anoikis resistance is regulated by ZC3H4 (Figure 8). Thus, a combination therapy targeting key inflammatory factors, growth-promoting factors, and epigenetic modifications may be the most successful strategy for treating highly complex and devastating fibrotic diseases.

Abbreviations

Flow cytometry= FCM; SiO_2= silicon dioxide; extracellular matrix= ECM; MCPIP1= monocyte chemotactic protein-1-induced protein 1; conditioned medium= CM; NTRK2= TrkB; HPF-a= human pulmonary fibroblasts-adult; endoplasmic reticulum stress= ERS; mouse pulmonary fibroblasts= MLG; MCP-1= monocyte chemoattractant protein-1; CCL2= C-C chemokine ligand 2; CCR2= C-C chemokine receptor 2; DMEM= Dulbecco's modified Eagle's medium; NS= normal saline; FBS= fetal bovine serum; NGS= normal goat serum; BALF= bronchoalveolar lavage fluid; Principal component analysis= PCA; Poly-2-hydroxyethyl methacrylate= poly-HEMA;

Declarations

Acknowledgments

This study is the result of work that was partially supported by the resources and facilities at the Core Laboratory at the Medical School of Southeast University. This study is the result of work that was partially supported by resources and facilities at the Core Laboratory at the Medical School of Southeast University.

Author contributions

Y.J., L.Y., W.J. and Z.X. performed the experiments, interpreted the data, prepared the figures, and wrote the manuscript. L.W., W.S., D.J., H.J. and C.M. performed the experiments and interpreted the data. W.W. and F.S. designed the experiments, interpreted the data, and wrote the manuscript. J.C. provided laboratory space and funding, designed the experiments, interpreted the data, wrote the manuscript, and directed the project. All authors read, discussed, and approved the final manuscript.

Conflict of interest

The authors declare no conflict of interest.

Funding

This work was supported by the National Key R&D Program of China (2017YFA0104303) and the National Natural Science Foundation of China (Nos. 81972987, 81773796, and 81700068).

Availability of data and materials

All of the relevant raw data and materials are freely available to any investigator upon request.

Ethics approval and consent to participate

Not applicable

Consent for publication

Not applicable

References

1. Wynn TA. Integrating mechanisms of pulmonary fibrosis. The Journal of experimental medicine. 2011;208(7):1339–50.
2. Kuhn C, McDonald JA. The roles of the myofibroblast in idiopathic pulmonary fibrosis. Ultrastructural and immunohistochemical features of sites of active extracellular matrix synthesis. Am J Pathol. 1991;138(5):1257–65.
3. Douglas WW, Ryu JH, Schroeder DR. Idiopathic pulmonary fibrosis: impact of oxygen and colchicine, prednisone, or no therapy on survival. Am J Respir Crit Care Med. 2000;161(4 Pt 1):1172–8.
4. Martin-Medina A, Lehmann M, Burgy O, Hermann S, Baarsma HA, Wagner DE, De Santis MM, Ciolek F, Hofer TP, Frankenberger M, et al. Increased extracellular vesicles mediate WNT-5A signaling in idiopathic pulmonary fibrosis. Am J Respir Crit Care Med. 2018;198(12):1527–38.
5. Gilmore AP. Anoikis. Cell Death Differ. 2005;12:1473–7.
6. Meredith JE, Fazeli B, Schwartz MA. The extracellular matrix as a cell survival factor. Mol Biol Cell. 1993;4(9):953–61.
7. Hynes RO. The extracellular matrix: not just pretty fibrils. Science. 2009;326(5957):1216–9.
8. Wynn TA. Common and unique mechanisms regulate fibrosis in various fibroproliferative diseases. J Clin Invest. 2007;117(3):524–9.
9. Rennebeck G, Martelli M, Kyprianou N. Anoikis and survival connections in the tumor microenvironment: is there a role in prostate cancer metastasis? Cancer Res. 2005;65(24):11230–5.
10. Simpson CD, Anyiwe K, Schimmer AD. Anoikis resistance and tumor metastasis. Cancer Lett. 2008;272(2):177–85.
11. Xie X, Zhu T, Chen L, Ding S, Chu H, Wang J, Yao H, Chao J. MCPIP1-induced autophagy mediates ischemia/reperfusion injury in endothelial cells via HMGB1 and CaSR. Sci Rep. 2018;8(1):1735.
12. Wang X, Zhang Y, Zhang W, Liu H, Zhou Z, Dai X, Cheng Y, Fang S, Yao H, Chao J. **MCPIP1 regulates alveolar macrophage apoptosis and pulmonary fibroblast activation after** *in vitro* **exposure to silica**. Toxicol Sci. 2016;151(1):126–38.
13. Yang X, Wang J, Zhou Z, Jiang R, Huang J, Chen L, Cao Z, Chu H, Han B, Cheng Y, et al. Silica-induced initiation of circular ZC3H4 RNA/ZC3H4 pathway promotes the pulmonary macrophage activation. FASEB J. 2018;32(6):3264–77.
14. Ruan X, Schneck H, Schultz S, Fehm T, Cahill MA, Seeger H, Chen R, Yu Q, Mueck AO, Neubauer H. Nomegestrol acetate sequentially or continuously combined to estradiol did not negatively affect membrane-receptor associated progestogenic effects in human breast cancer cells. Gynecol Endocrinol. 2012;28(11):863–6.
15. Liu H, Dai X, Cheng Y, Fang S, Zhang Y, Wang X, Zhang W, Liao H, Yao H, Chao J. MCPIP1 mediates silica-induced cell migration in human pulmonary fibroblasts. Am J Physiol Lung Cell Mol Physiol.

2016;310(2):L121–32.

16. Jiang R, Zhou Z, Liao Y, Yang F, Cheng Y, Huang J, Wang J, Chen H, Zhu T, Chao J. The emerging roles of a novel CCCH-type zinc finger protein, ZC3H4, in silica-induced epithelial to mesenchymal transition. Toxicol Lett. 2019;307:26–40.
17. Zhang P, Chen L, Song Y, Li X, Sun Y, Xiao Y, Xing Y. Tetraiodothyroacetic acid and transthyretin silencing inhibit pro-metastatic effect of L-thyroxin in anoikis-resistant prostate cancer cells through regulation of MAPK/ERK pathway. Exp Cell Res. 2016;347(2):350–9.
18. Giménez A, Duch P, Puig M, Gabasa M, Xaubet A, Alcaraz J. Dysregulated collagen homeostasis by matrix stiffening and TGF-β1 in fibroblasts from idiopathic pulmonary fibrosis patients: role of FAK/Akt. Int J Mol Sci. 2017;18(11):2431.
19. Demers MJ, Thibodeau S, Noel D, Fujita N, Tsuruo T, Gauthier R, Arguin M, Vachon PH. Intestinal epithelial cancer cell anoikis resistance: EGFR-mediated sustained activation of Src overrides fak-dependent signaling to MEK/Erk and/or PI3-K/Akt-1. J Cell Biochem. 2009;107(4):639–54.
20. Liu H, Fang S, Wang W, Cheng Y, Zhang Y, Liao H, Yao H, Chao J. Macrophage-derived MCPIP1 mediates silica-induced pulmonary fibrosis via autophagy. Part Fibre Toxicol. 2016;13(1):55.
21. Liu H, Cheng Y, Yang J, Wang W, Fang S, Zhang W, Han B, Zhou Z, Yao H, Chao J, et al. BBC3 in macrophages promoted pulmonary fibrosis development through inducing autophagy during silicosis. Cell Death Dis. 2017;8(3):e2657.
22. Morimura N, Tezuka Y, Watanabe N, Yasuda M, Miyatani S, Hozumi N, Tezuka Ki K. Molecular cloning of POEM: a novel adhesion molecule that interacts with alpha8beta1 integrin. J Biol Chem. 2001;276(45):42172–81.
23. Brandenberger R, Schmidt A, Linton J, Wang D, Backus C, Denda S, Muller U, Reichardt LF. Identification and characterization of a novel extracellular matrix protein nephronectin that is associated with integrin alpha8beta1 in the embryonic kidney. J Cell Biol. 2001;154(2):447–58.
24. Sato Y, Uemura T, Morimitsu K, Sato-Nishiuchi R, Manabe R, Takagi J, Yamada M, Sekiguchi K. Molecular basis of the recognition of nephronectin by integrin alpha8beta1. J Biol Chem. 2009;284(21):14524–36.
25. Linton JM, Martin GR, Reichardt LF. The ECM protein nephronectin promotes kidney development via integrin alpha8beta1-mediated stimulation of Gdnf expression. Development. 2007;134(13):2501–9.
26. Fang S, Guo H, Cheng Y, Zhou Z, Zhang W, Han B, Luo W, Wang J, Xie W, Chao J. circHECTD1 promotes the silica-induced pulmonary endothelial-mesenchymal transition via HECTD1. Cell Death Dis. 2018;9(3):396.
27. Marangi M, Pistritto G. Innovative therapeutic strategies for cystic fibrosis: moving forward to CRISPR technique. Front Pharmacol. 2018;9:396.
28. Lee JM, Yoshida M, Kim MS, Lee JH, Baek AR, Jang AS, Kim DJ, Minagawa S, Chin SS, Park CS, et al. Involvement of alveolar epithelial cell necroptosis in idiopathic pulmonary fibrosis pathogenesis. Am J Respir Cell Mol Biol. 2018;59(2):215–24.

29. Piguet PF, Collart MA, Grau GE, Sappino AP, Vassalli P. Requirement of tumour necrosis factor for development of silica-induced pulmonary fibrosis. Nature. 1990;344(6263):245–7.
30. Richeldi L, Collard HR, Jones MG. Idiopathic pulmonary fibrosis. Lancet. 2017;389(10082):1941–52.
31. Paoli P, Giannoni E, Chiarugi P. Anoikis molecular pathways and its role in cancer progression. Biochim Biophys Acta. 2013;1833(12):3481–98.
32. Aslan B, Monroig P, Hsu MC, Pena GA, Rodriguez-Aguayo C, Gonzalez-Villasana V, Rupaimoole R, Nagaraja AS, Mangala S, Han H-D, et al. The ZNF304-integrin axis protects against anoikis in cancer. Nat Commun. 2015;6:7351.
33. Li K, Zhao G, Ao J, Gong D, Zhang J, Chen Y, Li J, Huang L, Xiang R, Hu J, et al. ZNF32 induces anoikis resistance through maintaining redox homeostasis and activating Src/FAK signaling in hepatocellular carcinoma. Cancer Lett. 2019;442:271–8.
34. Leung CC, Yu IT, Chen W. **Silicosis** *Lancet*. 2012;379(9830):2008–18.
35. Fujimura N. Pathology and pathophysiology of pneumoconiosis. Curr Opin Pulm Med. 2000;6(2):140–4.
36. Mandrioli D, Schlünssen V, Ádám B, Cohen RA, Colosio C, Chen W, Fischer A, Godderis L, Göen T, Ivanov ID, et al. WHO/ILO work-related burden of disease and injury: protocol for systematic reviews of occupational exposure to dusts and/or fibres and of the effect of occupational exposure to dusts and/or fibres on pneumoconiosis. Environ Int. 2018;119:174–85.
37. Sergent JA, Paget V, Chevillard S. Toxicity and genotoxicity of nano-SiO2 on human epithelial intestinal HT-29 cell line. Ann Occup Hyg. 2012;56(5):622–30.
38. Cullinan P, Reid P. Pneumoconiosis. Prim Care Respir J. 2013;22(2):249–52.
39. Uhal BD, Joshi I, True AL, Mundle S, Raza A, Pardo A, Selman M. **Fibroblasts isolated after fibrotic lung injury induce apoptosis of alveolar epithelial cells** *in vitro*. Am J Physiol. 1995;269(6 Pt 1):L819–28.
40. Cao Z, Xiao Q, Dai X, Zhou Z, Jiang R, Cheng Y, Yang X, Guo H, Wang J, Xi Z, et al. circHIPK2-mediated sigma-1R promotes endoplasmic reticulum stress in human pulmonary fibroblasts exposed to silica. Cell Death Dis. 2017;8(12):3212.
41. Uhal BD, Joshi I, Hughes WF, Ramos C, Pardo A, Selman M. Alveolar epithelial cell death adjacent to underlying myofibroblasts in advanced fibrotic human lung. Am J Physiol. 1998;275(6):L1192–9.
42. Zhou Y, Horowitz JC, Naba A, Ambalavanan N, Atabai K, Balestrini J, Bitterman PB, Corley RA, Ding BS, Engler AJ, et al. Extracellular matrix in lung development, homeostasis and disease. Matrix Biol. 2018;73:77–104.
43. Liu D, Ke Z, Luo J. Thiamine deficiency and neurodegeneration: the interplay among oxidative stress, endoplasmic reticulum stress, and autophagy. Mol Neurobiol. 2017;54(7):5440–8.
44. Verfaillie T, Salazar M, Velasco G, Agostinis P. Linking ER stress to autophagy: potential implications for cancer therapy. Int J Cell Biol. 2010;2010:930509.

45. Ghavami S, Yeganeh B, Zeki AA, Shojaei S, Kenyon NJ, Ott S, Samali A, Patterson J, Alizadeh J, Moghadam AR, et al. Autophagy and the unfolded protein response promote profibrotic effects of TGF-beta1 in human lung fibroblasts. Am J Physiol Lung Cell Mol Physiol. 2018;314(3):L493–504.
46. Romero F, Hong X, Shah D, Kallen CB, Rosas I, Guo Z, Schriner D, Barta J, Shaghaghi H, Hoek JB, et al. Lipid synthesis is required to resolve endoplasmic reticulum stress and limit fibrotic responses in the lung. Am J Respir Cell Mol Biol. 2018;59(2):225–36.
47. Son B, Kwon T, Lee S, Han I, Kim W, Youn H, Youn B. CYP2E1 regulates the development of radiation-induced pulmonary fibrosis via ER stress- and ROS-dependent mechanisms. Am J Physiol Lung Cell Mol Physiol. 2017;313(5):L916–29.
48. Nakajima S, Kitamura M. Bidirectional regulation of NF-kappaB by reactive oxygen species: a role of unfolded protein response. Free Radic Biol Med. 2013;65:162–74.

Figures

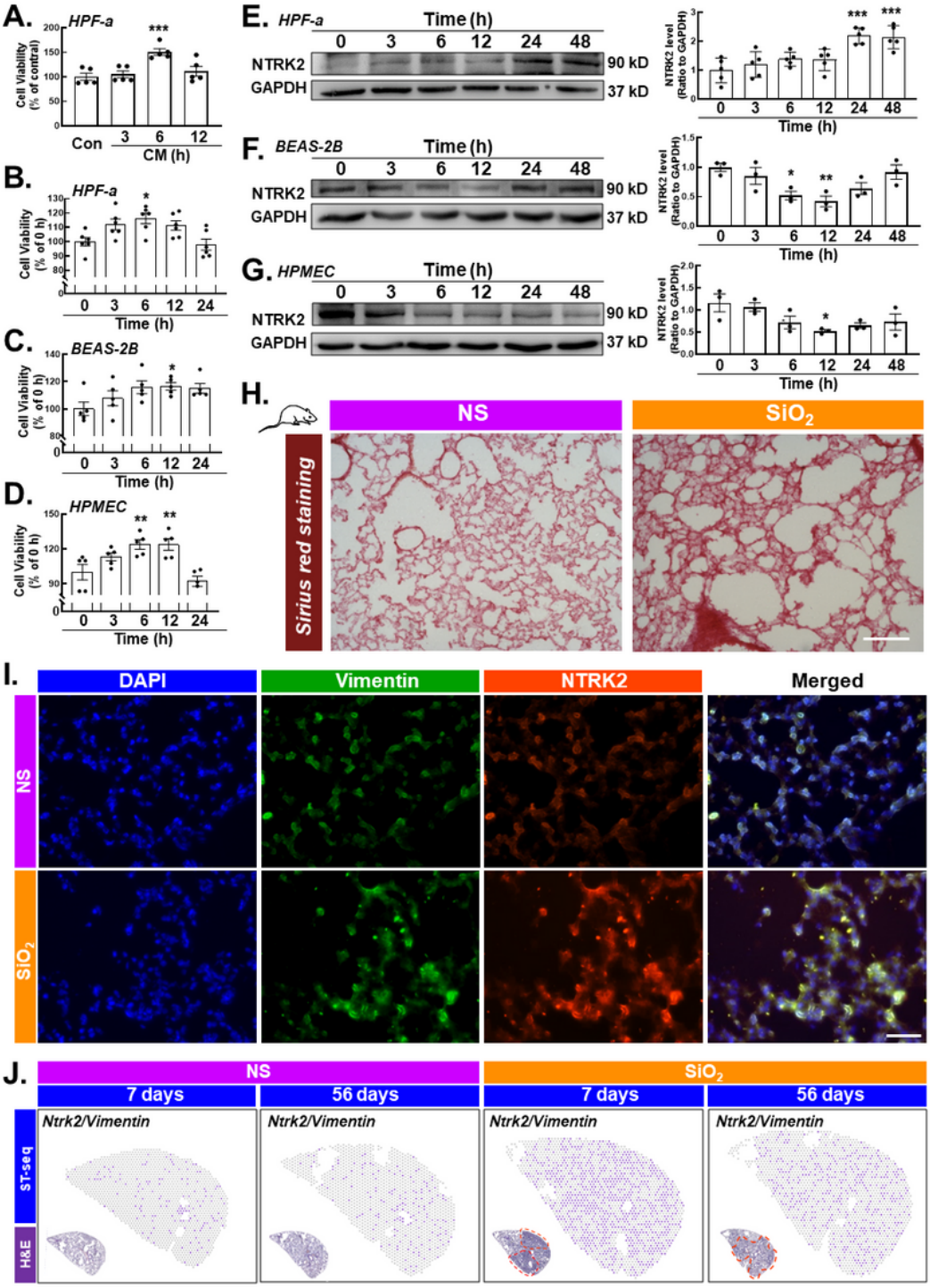

Figure 1

SiO2-induced pulmonary inflammation induced anoikis resistance only in HPF-a cells. (A). CCK-8 assay suggested that 6-h CM treatment significantly increased the viability of HPF-a cells (n=5); *P<0.05 vs. the control group. CM from macrophages treated with SiO2 increased the viability of HPF-a cells (B), BEAS-2B cells (C) and HPMECs (D), (n=5); *P<0.05 vs. the control group. Representative western blot and densitometric analyses of five separate experiments showing the effects of CM on the expression of the

anoikis resistance marker NTRK2 in HPF-a (E), BEAS-2B (F) and HPMEC (G); (n=5); *P<0.05 vs. the 0-h group, **P<0.01 vs. the 0-h group, ***P<0.001 vs. the 0-h group. (H). Sirius Red staining showed that SiO2 induced more collagen deposition and incomplete pulmonary alveoli in the lung tissues, indicating that the silicosis mouse model was successfully established. Scale bar=100 μm. (I). Immunofluorescence staining detected the expression of the fibroblast marker Vimentin and the anoikis protein NTRK2 in mouse lung tissue. Scale bar=100 μm. (J). Spatial transcriptomics showing the coexpression of Ntrk2 and Vimentin.

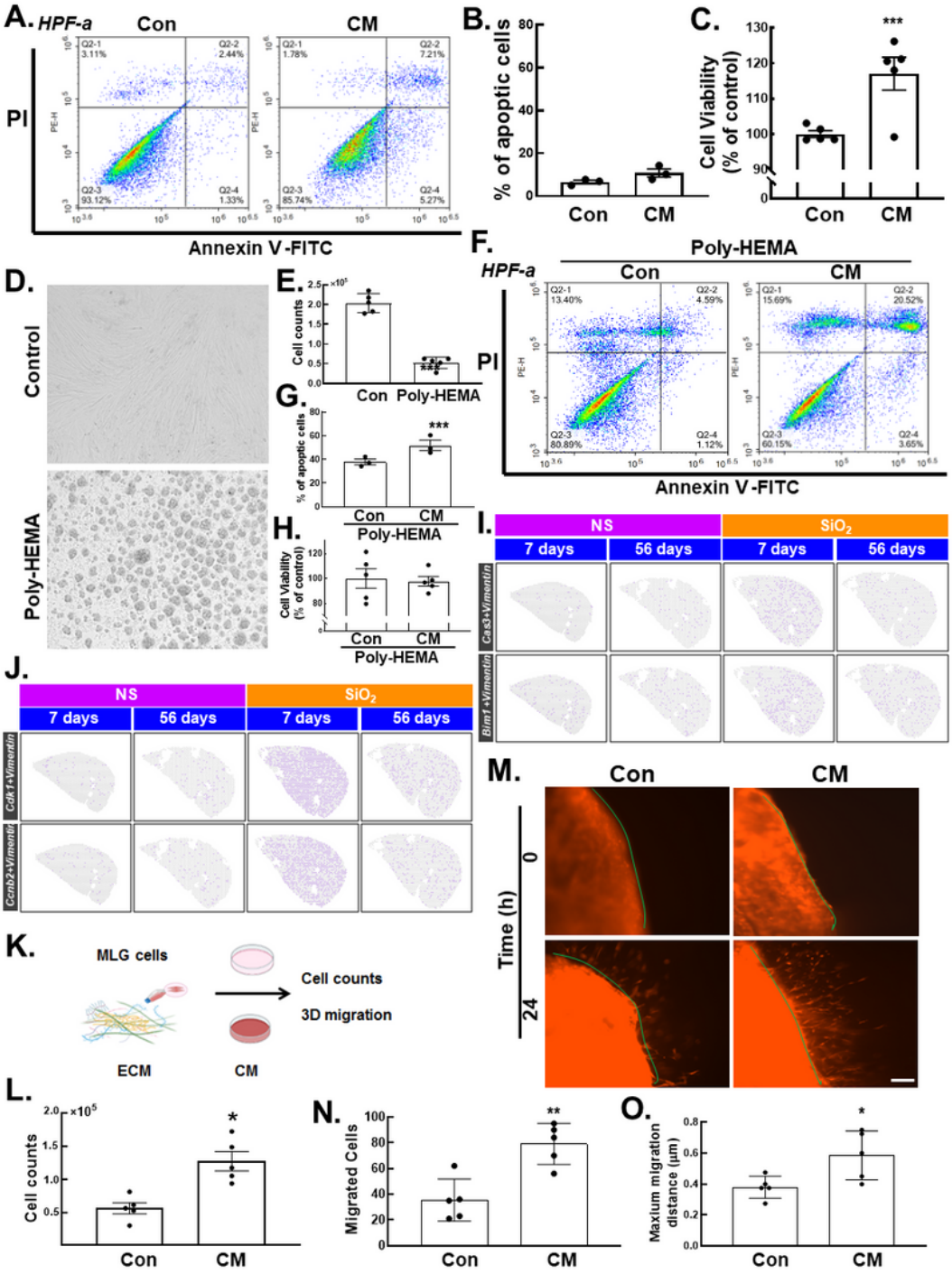

Figure 2

Anoikis resistance-mediated fibroblast activation in response to SiO2. (A). HPF-a cells were treated with CM for 24 h and double stained with Annexin V and PI. The sum of the counts in Q2-1, Q2-2 and Q2-4 was defined as the number of apoptotic cells. (B). Statistical analysis of three independent experiments of HPF-a cell apoptosis by FCM. (C). HPF-a cells treated with CM for 24 h and collected for counting. (n=5) ***P<0.001 vs. the control group. (D). Representative images showing the morphology of HFP-a cultured in wells pretreated with poly-HEMA. (E). HPF-a cells were suspended for 48 h and stimulated with CM for 6 h. According to the results of the CCK-8 assay, cell detachment induced by poly-HEMA attenuated the pulmonary inflammation-induced increase in the viability of HPF-a cells (n=5); ***P<0.001 vs. the control group. (F). HPF-a cells were suspended for 48 h before they were treated with CM for 24 h and double stained with Annexin V and PI. The sum of the counts in Q2-1, Q2-2 and Q2-4 was defined as the number of apoptotic cells. (G). Statistical analysis of three independent experiments of HPF-a cell apoptosis by FCM; ***P<0.001 vs. the attached group. (H). HPF-a cells were suspended for 48 h before they were treated with CM for 24 h and collected for counting. (n=5). (I). Spatial transcriptomics showed the coexpression of apoptosis markers (Cas3 and Bim1) and Vimentin. (J). Spatial transcriptomics showing the co-expression of proliferation markers (Cdk1 and Ccnb2) and Vimentin. (K). Schematic diagram of transplanted fibroblasts to ECM after decellularization. (L). Cell counting showed the effect of CM on MLG cell proliferation cultured in ECM. (n=5) *P<0.05 vs. the control group. (M). It was observed in the 3D migration experiment that the migration of fibroblasts were enhanced after 24 h of exposure to CM. Scale bar=275 μm. (N-O). Statistical results of the number of migrating fibroblasts in the 3D migration experiment and the maximum migration distance after 24 h of exposure to CM (n=5). *P<0.05 vs. the control group, **P<0.01 vs. the control group.

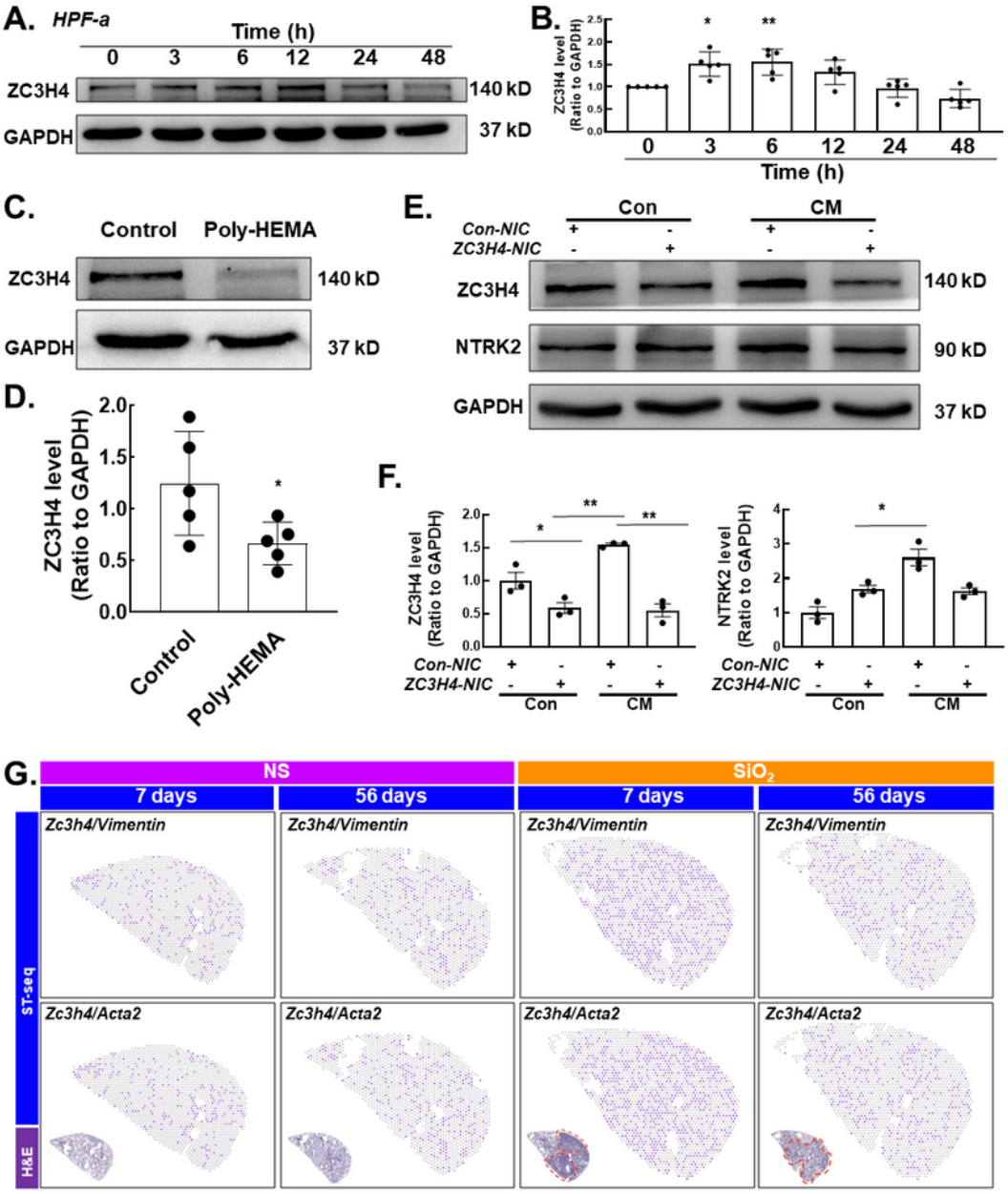

Figure 3

ZC3H4 is involved in anoikis resistance-mediated fibroblast activation in response to SiO2. (A). Representative western blot showing that macrophage-CM upregulated ZC3H4 expression in HPF-a cells. (B). Densitometric analyses of five separate experiments suggested that macrophage-CM upregulated ZC3H4 expression in HPF-a cells (n=5); *P<0.05 vs. 0 h, **P<0.001 vs. 0 h. (C). Representative western blot analysis suggested that poly-HEMA attenuated CM-induced increases in ZC3H4 expression in HPF-a

cells. (D). Densitometric analyses of five separate experiments. (n=5); *P<0.05 vs. the control group. (E). Representative western blot showing the effects of ZC3H4-NIC transfection on ZC3H4 and NTRK2 expression in HPF-a cells. (F). Densitometric analyses of three separate experiments suggested that ZC3H4 NIC transfection affected CM-induced increases in ZC3H4 and TrkB expression in HPF-a cells (n=3); *P<0.05 vs. the corresponding control group, **P<0.001 vs. the corresponding control group. (G). Spatial transcriptomics showing the coexpression of Zc3h4 and Vimentin.

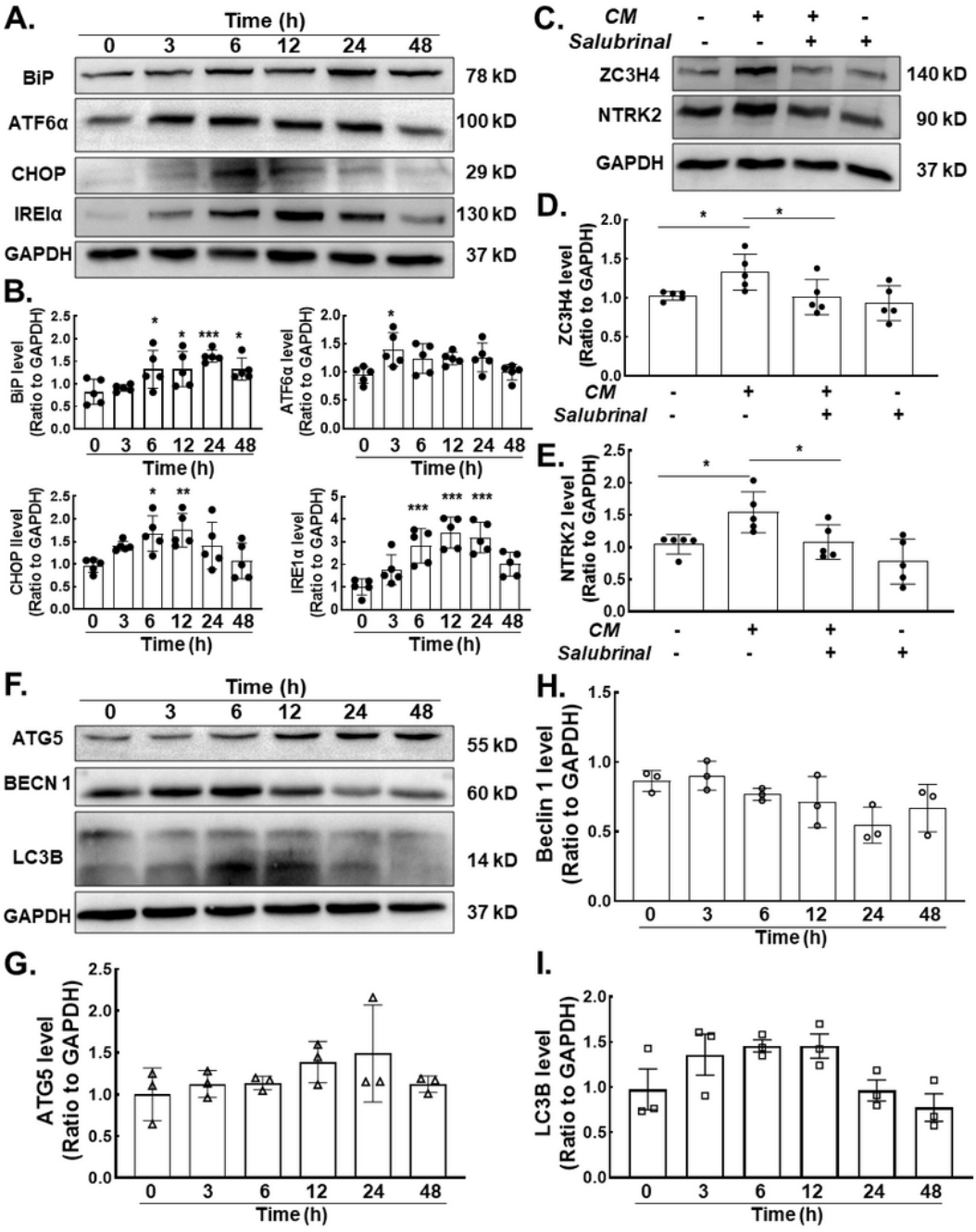

Figure 4

SiO2-induced pulmonary inflammation induces ERS and autophagy in HPF-a cells. (A). Representative western blot showing that macrophage-CM upregulated ERS-related protein expression in HPF-a cells. (B). Densitometric analyses of five separate experiments (n=5); *P<0.05 vs. 0 h, **P<0.01 vs. 0 h, ***P<0.001 vs. 0 h. (C). HPF-a cells were treated with salubrinal (an ERS inhibitor) for 6 h, and western blot analysis showed that ZC3H4 and NTRK2 expression was downregulated in response to salubrinal treatment. (D-E). Densitometric analyses of five separate experiments (n=5); *P<0.05 vs. control. (F). Representative western blot showing that macrophage-CM upregulated autophagy-related protein expression in HPF-a cells. (G-I). Densitometric analyses of five separate experiments (n=3).

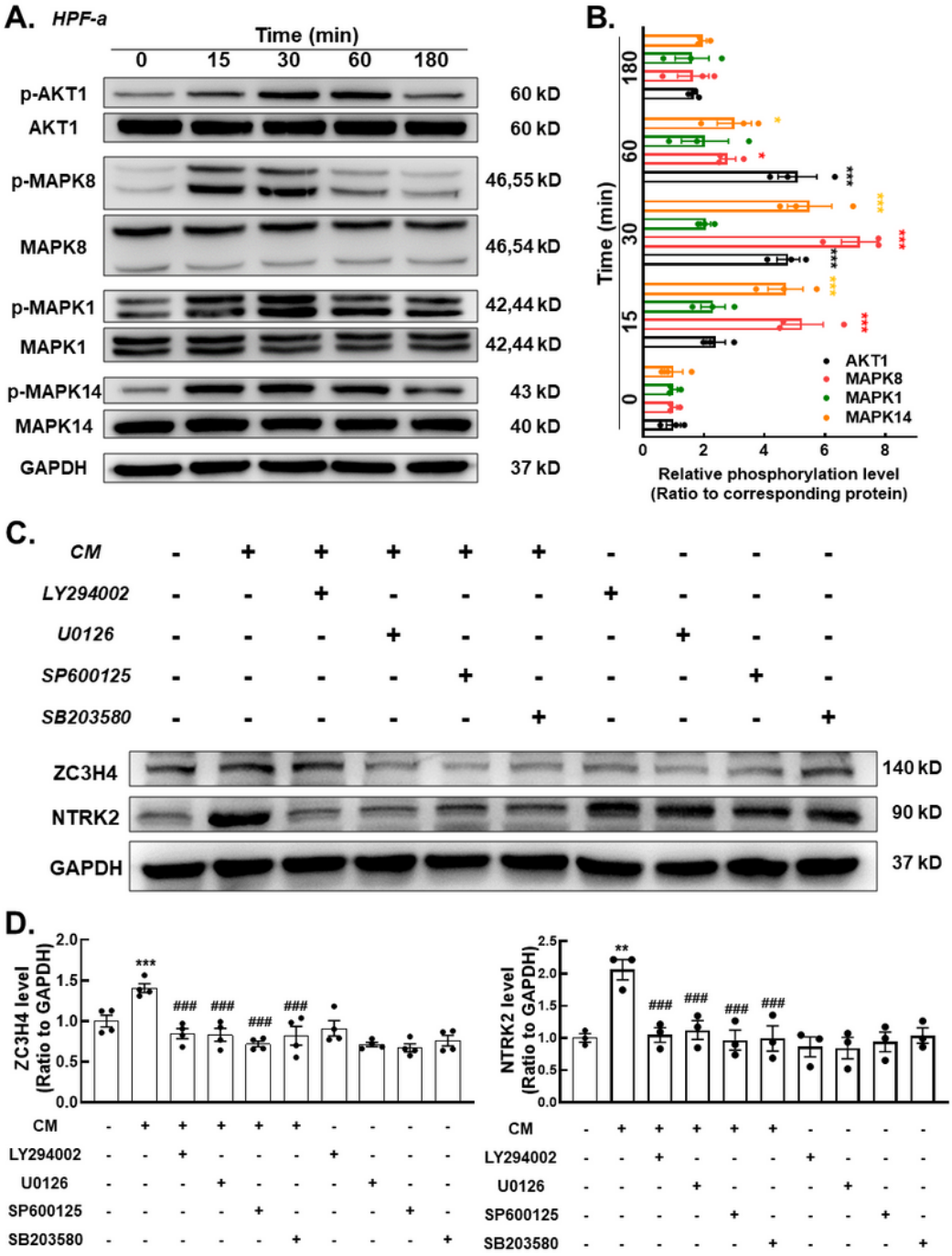

Figure 5

PI3K/MAPK signaling are involved in ZC3H4-mediated anoikis resistance in response to SiO2. (A). Representative western blot showing that macrophage-CM upregulated PI3K/MAPK-related protein expression in HPF-a cells. (B). Densitometric analyses of three separate experiments indicated that macrophage-CM upregulated the levels of phosphorylated Akt, JNK, Erk, and P38 in HPF-a cells (n=3); *P<0.05 vs. the corresponding protein level at 0 h, ***P<0.001 vs. the corresponding protein level at 0 h..

(C). Representative western blot showing that CM-induced ZC3H4 and NTRK2 expression was attenuated by pretreatment of HPF-a cells with a MAPK or PI3K/Akt inhibitor. (D). Densitometric analyses of ZC3H4 expression from 4 separate experiments and TrkB expression from 3 separate experiments. **P<0.01 vs. the corresponding control group, ***P<0.001 vs. the corresponding control group; ###P<0.001 vs. the corresponding CM group.

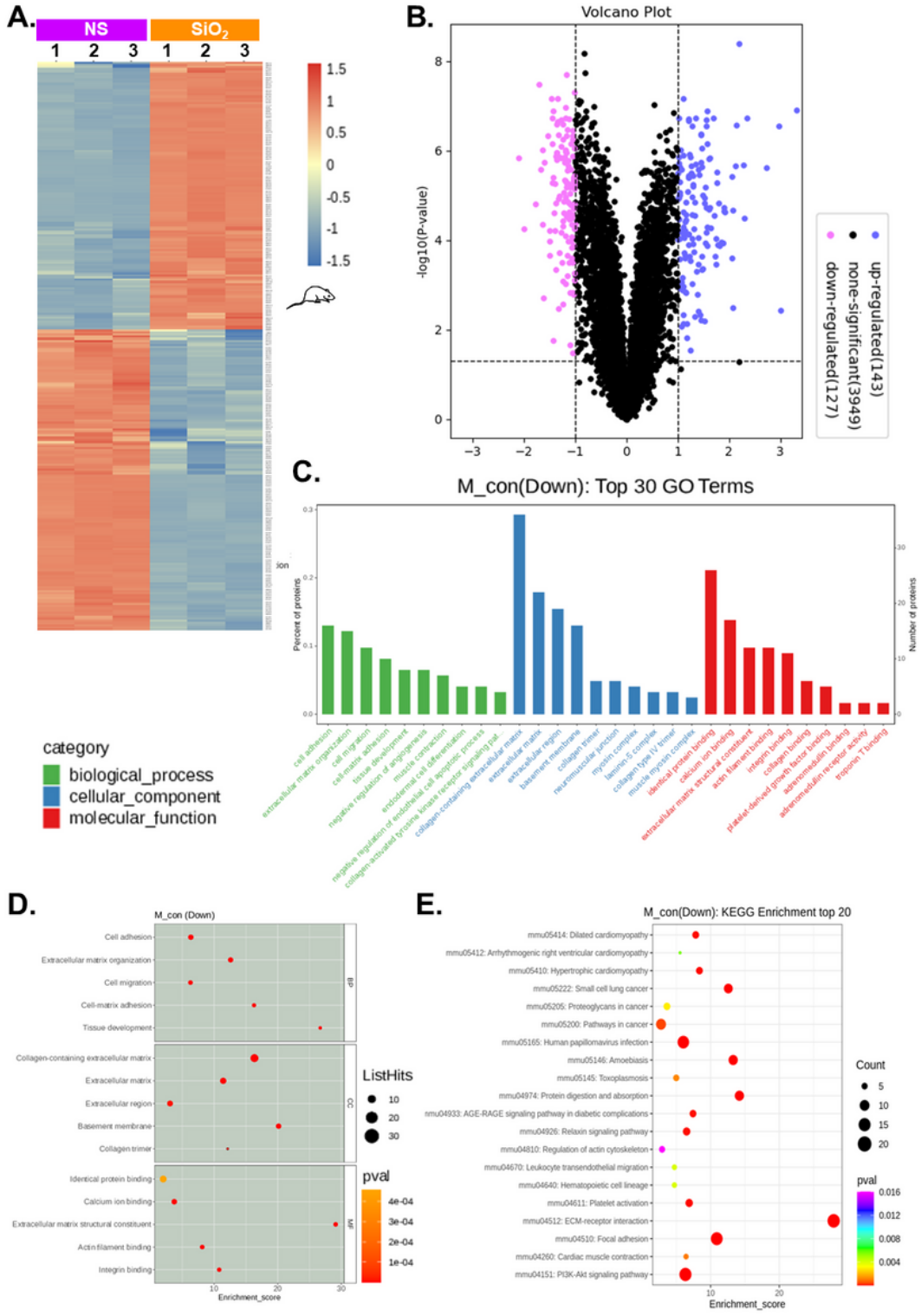

Figure 6

The ECM is involved in the detachment of lung fibroblasts in SiO2-induced pulmonary inflammation. (A-B) According to the ECM proteomics results, 270 proteins showed differential expression (143 proteins upregulated; 127 proteins downregulated) in ECM derived from lung tissues of silicosis model mice (n=3) with a FC =2. (C-D) GO analysis of the identified downregulated proteins: the top 30 GO entries were mainly involved in the biological process of cell adhesion, the major components were related to collagen, and molecular function was mainly associated with the recognition of protein binding. (E) KEGG analysis of the downregulated proteins: Among the top 20 enriched signaling pathways, mediating ECM receptor recognition and adhesion-related signaling were the most enriched pathways.

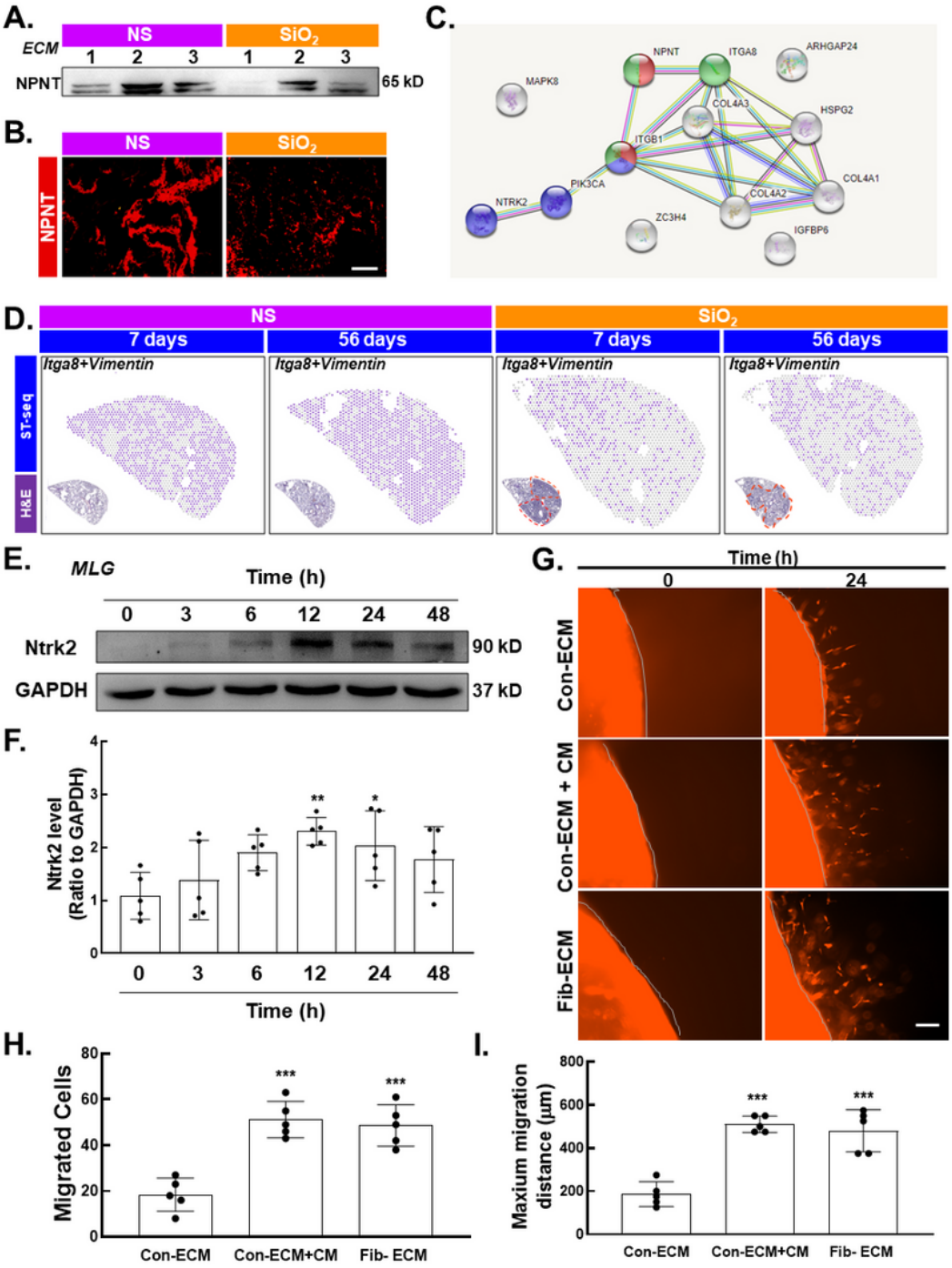

Figure 7

Detachment and apoptotic resistance of lung fibroblasts occurred independent of SiO2-induced pulmonary inflammation. (A) Representative western blot results showed downregulation of NPNT expression in ECM protein samples. (B) Immunofluorescence staining was used to detect the differential expression of NPNT in acellular ECM. Scale bar = 20 μm. (C). Protein-protein interaction network of the signaling pathways downstream of NPNT. (D). Spatial transcriptomics showing the coexpression of Itga8

and Vimentin. (E). Representative western blot analysis suggested that CM upregulated NTRK2 expression in MLG cells. (F). Densitometric analyses of five separate experiments suggested that CM upregulated NTRK2 expression in MLG cells. (n=5); *P<0.05 vs. ZC3H4 expression at 0 h, **P<0.01 vs. ZC3H4 expression at 0 h. (G). It was observed in the 3D migration experiment that the migration of fibroblasts were enhanced after 24 h both in ECM (from NS treated mouse) exposure to CM and in ECM from mouse treated SiO2 for 56 days. Scale bar=275 μm. (H-I). Statistical results of the number of migrating fibroblasts in the 3D migration experiment and the maximum migration distance after 24 h of exposure to CM (n=5). ***P<0.05 vs. the control group.

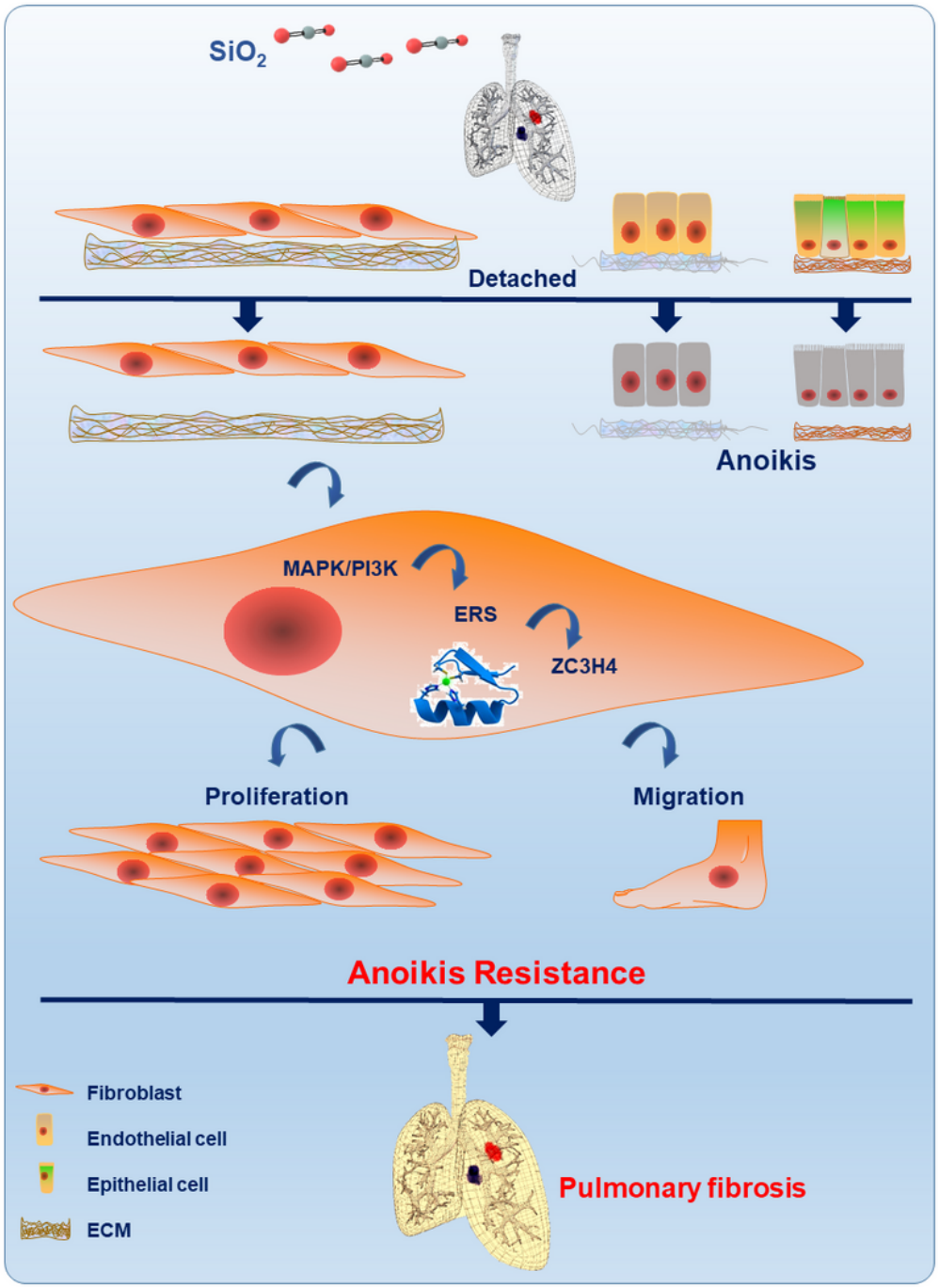

Figure 8

The mechanism of anoikis resistance induced by SiO2-mediated pulmonary inflammation in fibroblasts. In fibroblasts exposed to SiO2, adhesion to the ECM was weakened, and detachment occurred. In addition, the prosurvival signaling pathway PI3K/MAPK was activated, which subsequently led to increased ZC3H4 expression, which enhances anoikis resistance in fibroblasts. Apoptotic resistance of

fibroblasts and activation of differentiated myofibroblasts resulted in enhanced proliferation and migration and increased collagen synthesis.

Supplementary Files

This is a list of supplementary files associated with this preprint. Click to download.

- 2019AnoikissuppleLYv4.docx